Local Effective Crystal Field Combined with Molecular Mechanics. Improved QM/MM Junction and Application to Fe(II) and Co(II) Complexes

M. B. Darkhovskii[†] and A. L. Tchougréeff*[,†,‡]

L.Y. Karpov Institute of Physical Chemistry, Vorontsovo Pole 10, 105064 Moscow, Russia, and Center for Computational Chemistry at the M. V. Keldysh Institute for Applied Mathematics of RAS Miusskaya Pl. 4a, 125047 Moscow, Russia

Received: September 3, 2003; In Final Form: January 16, 2004

The quantum mechanical effective Hamiltonian of crystal field (EHCF) methodology (previously developed for describing electronic structure of transition metal complexes) is combined with the Gillespie−Kepert version of molecular mechanics (MM) in order to describe multiple potential energy surfaces (PES) of the Werner-type complexes corresponding to different spin states of the latter. The procedure thus obtained is a special version of the hybrid quantum mechanics/molecular mechanics approach. The MM part is responsible for representing the whole molecule, including ligand atoms and metal ion coordination sphere, but leaving aside the effects of the d shell. The quantum mechanics part (EHCF) is restricted to the metal ion d shell. The method reproduces with considerable accuracy geometry and spin states of a wide range of Fe(II) and Co(II) complexes of various total spin and coordination polyhedra and containing both monodentate and polydentate ligands with aliphatic and aromatic nitrogen donor atoms. In this setting, a single MM parameters set is shown to be sufficient for dealing with all spin states and coordination numbers of the complexes.

1. Introduction

Economical computational tools suitable for estimations of electronic structure and molecular geometry of transition metal complexes (TMC) are highly in demand. The molecular mechanics (MM)[1] both itself and in the molecular dynamics setting is intensely used in calculations of proteins and other polyatomic organic molecules. During the past decade, a considerable number of attempts were made to apply the conventional MM scheme to the metal ion complexes with organic ligands.[2−11] The main problem here is that in TMCs several electronic states may occur in a narrow energy range close to its ground state. Sometimes, the potential energy surfaces (PESs) corresponding to different electronic terms of the metal ion d shell intersect which results in spin transitions.[12] In organic molecules, this problem normally does not appear and the MM description is valid since electronically excited states are well separated from the respective ground state on the energy scale. In these cases, a single quantum state of the electronic system suffices for the description of a molecule. Clearly, this is not mandatorily true for TMCs.

Also, within MM, it is hard to get an adequate modeling of the coordination sphere, in particular, to account for the flexibility of coordination polyhedron. The most straightforward way is to describe deformations of valence angles involving metal atom at the vertex with potential functions more sophisticated than harmonic potentials. Also a so-called points-on-a-sphere (POS) approach was proposed.[13,14] It suggests the shape of the coordination polyhedron to be ultimately dictated by the inter-ligand van der Waals-like interactions. Recently, it has been shown[15,16] that it may be further improved by considering not the inter-ligand interaction (described through common non-bonding 6−12 or 6-exp potentials) but repulsion of effective interacting centers placed somewhere on the coordination bonds. This repulsion is suggested by the well-known qualitative theory by Gillespie[17] and formulated quantitatively by Kepert.[18] The approach recently brought insight of coordination geometries diversity. It allows a proper description of many cases of significant distortion in coordination geometry (for discussion and examples see refs 15 and 16). However, being an MM method, it is unable (and obviously not designed) to describe spin states of coordination compounds, which is necessary to discuss magnetic properties, as well as to provide correct estimates for energetics of a large number of important chemical and biochemical processes where they take part.

To incorporate electronic effects of the partially filled d shell in TMC's into the general MM scheme it was proposed in refs 19−23 to include the energy of the d shell as a separate contribution to the energy. It is done in variance with works[7,24,25] where the accent is put on estimating the spectral characteristics of the d shell at the geometry assessed with use of an MM treatment. Including the energy of the d shell explicitly allows us to account for electronic structure influence on the geometry of TMC. These are quantum effects specific for the open d shell which appear due to possible degeneracies of different electronic terms of the latter at certain complex geometries. Experimentally, this would correspond to the Jahn−Teller complexes and to spin active complexes. However, the ligand field energy in refs 7, 19, 22, 24, and 25 depends only on the distance between the metal ion and ligand donor atoms, which seems to be an oversimplified picture since the effects of the lone pair orientation on the ligand field must be taken into account.

Promising methods for quantitative estimates on TMCs are proposed in the framework of the hybrid quantum mechanics/molecular mechanics (QM/MM) methodology.[26−29] Most of their applications belong however to the organometallic realm

* To whom correspondence should be addressed. Karpov Institute of Physical Chemistry, Vorontsovo Pole 10, 105064 Moscow, Russia. Fax: +7-(095)-975-2450.

† L.Y. Karpov Instituteof Physical Chemistry.

‡ M. V. Keldysh Institute for Applied Mathematics.

10.1021/jp036622z CCC: $27.50
Published on Web 07/02/2004

or to that of complexes of heavy (second and third transition row) metals, without addressing different spin states within a calculation. In the frame of these attempts, a rather large part of the TMC is treated by a QM method leaving to MM only the periphery of the molecule, thus producing a computationally expensive description of the TMC structure. The QM methods used in the QM/MM hybrid schemes for the TMCs are most often based on the SCF approach. It is so for first of all[28,29] or the semiempirical level of the theory.[26] However, the SCF theory does not apply to the TMCs as thoroughly discussed in ref 43. The source of the problem is the strong correlation of electrons in the d shell resulting in an instability of Hartree−Fock problem solutions for the electronic structure of TMCs. Semiempirical methods have been proposed recently for electronic structure calculations of TMCs, such as SAM1,[30] MNDO/d,[31] and PM3-(tm)[32] employing the NDDO parametrization scheme. However, MNDO/d is not parametrized for the transition metals with only the exception of Zn. These methods suffer from the defects and insufficiency of the SCF scheme as well when applied to TMC with different spin states. For example, in the work in ref 33, substituted imidazole-like inhibitors binding to cytochrome P-450 are modeled by protoporphyrin IX ferric ion with ethyl sulfide as a constant second axial ligand. The binding energy is calculated by the method in ref 30. There the molecule contains the metal ion in the doublet state, and the RHF calculation is used. However, for some ligands in the SCF UHF calculation, a spin-contaminated state is obtained. Also, optimized geometries of some complexes differ strongly from the experimental ones: for water the calculated distance, Fe−O is smaller than experimental by 0.5 Å, whereas for 3-phenylimidazole, the calculated distance Fe−N is shorter by 0.15 Å. In the work in ref 34, a large set of nickel(II) both low- and high-spin complexes with square planar cyclotetraazo ligands are modeled by the PM3(tm) method, and the obtained differences between experimental and calculated distances are larger than 0.12 Å for low-spin complexes and 0.07 Å for high-spin complexes. The authors concluded that the PM3(tm) method is inapplicable at least to this class of complexes. Recently, in ref 35, a construction of energy profiles of the different spin states of the complex [*Fe*(*heme*)](Hys)CO depending on the CO separation from the plane of the heme ring has been performed combining the angular overlap model (AOM) and "diatomics-in-molecule" methods. This semiempirical method is parametrized by comparison with TDDFT curves for ground states of different total spin. However, it is known that the TDDFT approach only partially include correlation effects for the d shell of the transition metal ion, so the status of these results is unclear. From a general point of view, semiempirical methods based on the SCF methodology take into account correlation mainly by parametrization rather than by form of the wave function. Thus, having a parametrization capable of describing properly certain spin state of the transition metal ion may not result in a correct description of other spin states with a different contribution of correlations.

The valence bond approach to the metal bonding proposed in a series of works[36−38] is based on the concept of hybridization of *s*- and *d*-AOs of the metal atom in different ligand environments. These works explore a physical situation different from that in "first-row" TMC we are mainly concerned with. That of the works in refs 36−38 may be qualified as "organometallic" due to direct involvement of the d orbitals into valence bond formation which establishes corresponding conditions for possible hybridization schemes. By contrast, in the "first-row" TMCs, the d electrons must be qualified as "non-bonding" thus forming a relatively isolated group: the d shell relatively weakly affected by the environment.

In the papers in refs 39 and 40, we proposed and tested a hybrid QM/MM description of TMCs targeted at first transition row metal complexes. It is based on the general approach[41] to molecular electronic structure and potential energy, which makes it possible to apply the QM description to that part of molecule in which electronic terms are close on the energy scale and to use the MM description for the part where the electronic states remain distant in energy. In refs 39 and 40, a combination of the effective Hamiltonian of crystal field (EHCF) method[43] in its local version,[42] EHCF(L), with the MMGK procedure[16] has been proposed and implemented for a series of Fe(II) complexes with nitrogen-containing ligands. Within the EHCF(L) approach the effective crystal field is presented as a sum of lone pair contributions (see below). This allows for a detailed description of the ligand field dependence not only on the metal−ligand distance but also on the lone pair orientation with respect to the metal ion. In the present paper, we report further improvement of the EHCF(L) approach and the results of application of the enhanced hybrid method to molecular and electronic structure estimates for the series of Fe(II) and Co (II) complexes of low- and high-spin.

The paper is organized as follows. In the next section, we briefly review the basic features of the EHCF(L) method.[42,43] Next we describe the improved EHCF(L) approach taking into account the ligand polarization in TMC. The last section provides the parametrization and application of the EHCF(L)/MMGK approach to calculations of several complexes.

2. Hybrid EHCF(L)/MM Model

The key point for incorporation of transition metal ions (TMI) into MM is to estimate the energy of the d shell as a function of the ligand sphere composition and structure. In this section, we review working approximations based on the EHCF(L) theory[42] and propose the improved EHCF(L) method taking into account the ligand polarization.

2.1. Basics of the EHCF(L). The concept of separating electron variables is to be employed when a hybrid QM/MM method is developed:[41] electrons have to be divided into groups, some of the groups whose excited electronic states are accessible in the experiment are treated by a QM method, whereas the behavior of other groups whose excited electronic states lay high in energy (and are not accessible in experiment) are modeled with use of MM. In a TMC comprising one TMI and ligands around it, the basis of valence atomic orbitals (AOs) containing the 4s-, 4p-, and 3d-AOs of the metal atom (for a first transition row element) and those of the ligand atoms is according to ref 43 divided into the d system which contains only 3d orbitals of the TMI and the l system which contains 4s-, 4p-AOs of the TMI and the valence AOs of the ligand atoms. In the EHCF method,[43] it is shown that the d shell can be described by the effective QM Hamiltonian $H_{\mathrm{d}}^{\mathrm{eff}}$:

$$H_{\mathrm{d}}^{\mathrm{eff}} = \sum_{\mu\nu\sigma} U_{\mu\nu}^{\mathrm{eff}} d_{\mu\sigma}^{+} d_{\nu\sigma} + \frac{1}{2}\sum_{\mu\nu\rho\eta}\sum_{\sigma\tau} (\mu\nu|\rho\eta) d_{\mu\sigma}^{+} d_{\rho\tau}^{+} d_{\eta\tau} d_{\nu\sigma} \quad (1)$$

where μ, ν, ρ, and η are the 3d-AO indices and σ, τ are the spin projection indices, and the standard notation for the two-electron integral $(\mu\nu \mid \rho\eta)$ is used. The d electron Coulomb interaction term is inherited from the free ion, and the effective core attraction parameters $U_{\mu\nu}^{\mathrm{eff}}$ contain contributions from the Coulomb and the resonance interaction of the d and l systems

$$U_{\mu\nu}^{\text{eff}} = \delta_{\mu\nu}U_{\text{dd}} + W_{\mu\nu}^{\text{atom}} + W_{\mu\nu}^{\text{field}} + W_{\mu\nu}^{\text{cov}} \quad (2)$$

The term

$$W_{\mu\nu}^{\text{atom}} = \delta_{\mu\nu}\left(\sum_{\alpha\in s,p} g_{\mu\alpha}P_{\alpha\alpha}\right) \quad (3)$$

is the repulsion of electrons in the d shell from those in the 4s- and 4p-AOs of the metal, where μ, α are the indices of metal 3d- and 4s, 4p-AOs respectively, $\delta_{\mu\nu}$ is the Kronecker symbol, $g_{\mu\alpha}$ is the electron−electron interaction parameter, and $P_{\alpha\alpha}$ is the density matrix diagonal element. The term

$$W_{\mu\nu}^{\text{field}} = \sum_L Q_L V_{\mu\nu}^L \quad (4)$$

is the Coulomb potential $V_{\mu\nu}^L$ of d electrons interacting with the net charge Q_L on the Lth ligand atom, having the standard crystal field theory form.[44] The covalence part

$$W_{\mu\nu}^{\text{cov}} = -\sum_i \beta_{\mu i}\beta_{\nu i}\left(\frac{1-n_i}{\Delta E_{\text{di}}} - \frac{n_i}{\Delta E_{i\text{d}}}\right) \quad (5)$$

ultimately comes from the resonance interaction between the d and l systems, where $\beta_{\mu i}$ ($\beta_{\nu i}$) are the resonance integrals between μth (νth) AO of the d shell and ith MO of the l system, ΔE_{di} ($\Delta E_{i\text{d}}$) is the charge-transfer energy from the d shell to the ith MO or backward, n_i (=0 and 1) is the occupation number of the ith MO. Summation here is extended to the canonical MOs (CMO) of the entire l system. This is the essence of the EHCF method.[43] The procedure expressed by eqs 1−5 has been shown to be able to reproduce the splitting of d shell levels with a 10% precision.[43−49]

In our papers,[39,42] we have derived and tested a local version of the EHCF method EHCF(L). It was shown that the splitting parameter 10*Dq* can be estimated with the error not exceeding 0.1 eV (this accuracy compares to that of the EHCF method itself) by the formula

$$W_{\mu\nu}^{\text{cov}} = \sum_\Lambda \sum_{L\in\Lambda} \beta_{\mu L}\beta_{\nu L} G_{LL}^{\text{adv}}(A_{\text{d}}) \quad (6)$$

where Λ enumerates the ligands, the subscripts L enumerate the one-electron local states referring to the lone pairs (LPs) residing on the donor atoms, and $\beta_{\mu\text{L}}$ is the resonance integral between the μth AO of the d shell and the Lth LP. The advanced Green's function $G_{LL}^{\text{adv}}(\epsilon)$ for the local state L in eq 6 is given by

$$G_{LL}^{\text{adv}}(\epsilon) = -\sum_i \frac{n_i {c_{iL}}^2}{\epsilon - (g_{\text{di}} - \epsilon_i)} \quad (7)$$

where c_{iL} is the coefficient of the LPs expansion over CMOs obtained by the max Ψ^4 localization procedure,[50] g_{di} is the interaction energy between d electron and electron on the ith MO, and ϵ_i is the energy of the ith CMO of the l system in the TMC.

The resonance integrals $\beta_{\mu L}$ in eq 6 can be expressed through the $\mathbf{t}^L$ vector of the resonance integrals between the metal d-AOs and the Lth LMO taken in the diatomic coordinate frame (DCF) related to the ligand Λ

$$\beta_{\mu L} = \sum_{\lambda L\in\Lambda} R_{\lambda\mu}{}^\Lambda t_\lambda^L \quad (8)$$

where the coefficients $R_{\lambda\mu}^\Lambda$ form a unitary matrix $\boldsymbol{R}^\Lambda$ transforming d orbitals from the global (laboratory) coordinate frame (GCF) to the DCF. The latter is defined so that its z axis is the straight line connecting the metal atom with the ligand donor atom.

Then, introducing the quantities

$$e_{\lambda\lambda'}{}^\Lambda = \sum_{L\in\Lambda} t_\lambda^L G_{LL}^{\text{adv}}(A_{\text{d}}) t_{\lambda'}^{L+} \quad (9)$$

we obtain

$$W_{\mu\nu}^{\text{cov}} = \sum_{\Lambda\lambda\lambda'} R_{\mu\lambda}{}^\Lambda e_{\lambda\lambda'}{}^\Lambda R_{\nu\lambda'}{}^\Lambda \quad (10)$$

where the matrix elements $e_{\lambda\lambda'}{}^\Lambda$ of the e^Λ matrix in the DCF are labeled by the indices $\lambda\lambda'$ taking values σ, π_x, π_y, δ_{xy},$\delta_{x_2-y_2}$ according to the symmetry of the metal *d*-orbitals with respect to the z axis of the DCF.

The expression eq 9 defines the $e_{\lambda\lambda'}^\Lambda$ parameters in terms of the quantities which can be calculated within the EHCF(L) method. Their relation with the standard AOM[51] is described in details in ref 42. There eqs 9 and 10 have been used to calculate the values of the e_σ and e_π parameters for a series of octahedral complexes with nitrogen containing ligands. That calculation was in a good agreement with experimental 10*Dq* values (within 10% accuracy).

2.2. Perturbative Estimates of Ligands' Electronic Structure Parameters. In section 2.1, we reviewed the EHCF(L) theory which allows to estimate the crystal field in terms of local electronic structure parameters (ESP) of the ligands. By this method, it can be done for arbitrary geometry of the complex, which is prerequisite for developing a hybrid QM/MM method.

The natural way to go further with this technique is to apply the perturbation theory to obtain estimates of the l system Green's function entering eqs 6 and/or 9. It was assumed and reasoned in ref 39 that the bare Green's function for the l system has a block-diagonal form

$$\boldsymbol{G}_{00}^{\text{l}} = \oplus_\Lambda \boldsymbol{G}_0^\Lambda \quad (11)$$

Nonvanishing blocks $\boldsymbol{G}_0^\Lambda$ correspond to separate ligands (fragments) Λ containing the unperturbed diagonal Green's function matrix elements $(G_0^\Lambda)(\epsilon)_{LL}^{\text{adv}}$ corresponding to the LP L located on the ligand Λ

$$(G_0^\Lambda(\epsilon))_{LL}^{\text{adv}} = \sum_{i\in\Lambda} \lim_{\delta\to 0^+} \frac{(c_{iL}{}^\Lambda)^2 n_i}{\epsilon - \epsilon_{\Lambda i}{}^{(0)} + i\delta} \quad (12)$$

where c_{iL}^Λ is the same expansion coefficient as in eq 7 but for the LP of the separate ligand Λ, and $\epsilon_{\Lambda i}{}^{(0)}$ is the ith MO energy of that same free ligand. Then the eq 6 contains Green's function $(G_0^\Lambda)(\epsilon)_{LL}^{\text{adv}}$ of the free ligand and the summations in eq 6 is performed over the separate ligands Λ and their LPs indexed as L.

The Coulomb interaction between the ligands themselves and between each of them and the metal ion when turned on does not break the block diagonal structure of the bare Green's function $\boldsymbol{G}_{00}^{\text{l}}$. Then the approximate Green's function for the l system conserves the form eq 11 but with the poles now corresponding to the orbital energies of the ligand molecules in the Coulomb field induced by the central ion and by other ligands ($\Lambda' \neq \Lambda$) rather than to those of the free ligands.

In the following subsection, we consider an implementation of this approach taking into account the Coulomb field effects and thus allowing us to express the Green's function of the l system in terms of the Green's functions of separate ligands.

2.3. Approximate Treatment of the l System Electronic Structure. *2.3.1. Rigid Ligands' MOs Model.* The simplest picture of the influence of the central ion on the surrounding ligands reduces to that of the Coulomb field affecting the positions of the poles of the Green's function (orbital energies) of the free ligand. The form of the CMOs of each ligand is left unchanged which is a picture of the rigid ligands' MOs (RLMO) ref 39. According to ref 52, the effect of the Coulomb field upon the orbital energies is represented by

$$(G^{\Lambda})^{-1} = (G_0^{\Lambda})^{-1} - \Sigma^{(f)} \tag{13}$$

where G_0^{Λ} is the Green's function for the free ligand and the self-energy term $\Sigma^{(f)}$ is due to the external Coulomb field. The perturbed Green's function G^{Λ} within the first order has the same form as G_0^{Λ} but its poles are expressed through the orbital energies of the free ligand $\epsilon_i^{(0)}$ and the self-energy parts $\Sigma_{ii}^{(f)}$

$$\epsilon_i = \epsilon_i^{(0)} + \Sigma_{ii}^{(f)} \tag{14}$$

The self-energy $\Sigma_{ii}^{(f)}$ is taken as that of a pure electrostatic interaction between the partial electron densities and effective point atomic charges by

$$\Sigma_{ii}^{(f)} \approx \sum_{N\in\Lambda} \rho_{iN}\delta h_N \tag{15}$$

where ρ_{iN} is the partial electron density of the ith CMO of the ligand Λ on the Nth atom of the ligand

$$\rho_{iN} = \sum_{\alpha\in N} c_{i\alpha}{}^2 \tag{16}$$

where $c_{i\alpha}$ are the ith MO LCAO coefficients of the free ligand, and the core Hamiltonian perturbation δh_N is

$$\delta h_N = -e^2\left(\frac{(Z_M - n_d)}{R_N} + \sum_{\Lambda'\neq\Lambda N'\in\Lambda'} \frac{Q_{N'}}{R_{NN'}}\right) \tag{17}$$

The atomic quantities δh_N are equal to the perturbations $\delta h_{\alpha\alpha}$ of the corresponding core Hamiltonian matrix elements in the ligand AO basis. This is like that since, within the CNDO approximation[53] accepted in ref 39, the quantities $\delta h_{\alpha\alpha}$ are the same for all $\alpha \in N$.

These formulas comprise the RLMO model of the electronic structure of the l system of the TMC. The RLMO procedure has been implemented in the program suite ECFMM 1.0.[54] Its application to analysis of molecular geometries are described in refs 39 and 40. Despite satisfactory results in geometry and spin states description of some iron(II) complexes, the main conclusion is that the crystal field is reproduced with too large an error due to the overestimated repulsion of d electrons from the ligands lone pairs. Due to that in refs 39 and 40, we had to scale correspondingly the Racah parameters differently for complexes with pyridine-like and amino nitrogen donor atoms, since in the latter analogous error was small. In the following subsection, we propose an improved model taking into account polarization effects in the ligand sphere which is able to describe both types of ligands within a unified parametrization.

2.3.2. Sparkle Model and Its Perturbative Versions. The model of electronic structure of TMC which considers the metal ion as a point charge equal to its oxidation degree or formal charge is habitually called the sparkle model.[55] Within models of that type, a semiempirical SCF calculation is performed for the ligands of the complex placed in the electrostatic field induced by the central ion with its formal charge ("sparkle"). Thus, the charge redistribution occurring in the ligands is obtained by performing a standard SCF procedure for them.

Within models of the sparkle family, the effect of the external Coulomb field does not reduce to the renormalization of the orbital energies as it is within the RLMO model (see above). The electron distribution also changes when the ligand molecules are put into the field. That means that the density matrix of the system varies and, accordingly, the effective point charges Q residing on the atoms of the molecule in eq 17 change. We will describe this situation by means of polarizability concept.[56] According to it, the difference between polarized and nonpolarized effective charge on atom A is

$$\delta Q_A = Q_A - Q_A^0 = \sum_B \Pi_{AB}\delta h_B = \sum_B \Pi_{AB}(\delta h_B^0 + \sum_{C\neq B} \Gamma_{AC}\delta Q_C) \tag{18}$$

where Π_{AB} is atomic mutual polarizability discussed below whereas $\delta h_A{}^0$ taken from eq 17 can be rewritten as

$$\begin{gathered} \delta h_A^0 = -Z_M\Gamma_{MA} - \sum_B Q_B^0\Gamma_{BA} \\ \Gamma_{MA} = e^2/R_{MA} \\ \Gamma_{AB} = (1 - \delta_{\Lambda\Lambda'})e^2/R_{AB}\ (A\in\Lambda;\ B\in\Lambda') \\ \sum_A \delta Q_A = \sum_A \sum_{\alpha\in A} \delta P_{\alpha\alpha} = 0 \end{gathered} \tag{19}$$

The quantities Q_B^0 in the above equation are the bare effective charges as they appear from the calculation on a free ligand to which the atom B belongs. The term δh_B^0 is renormalized due to the electron−electron interaction Γ_{AC} resulting in the true (renormalized or dressed) perturbation δh_B. The quantity δQ_A is the change of the effective atomic charge due to polarization, and $\delta P_{\alpha\alpha}$ is the change of the αth AO orbital density matrix element. In the matrix form, eq 18 reads

$$\begin{gathered} \delta\boldsymbol{Q} = \boldsymbol{Q} - \boldsymbol{Q}^0 = \Pi(\delta\boldsymbol{h}^0 + \Gamma\delta\boldsymbol{Q}) \\ \delta\boldsymbol{Q} = (1 - \Pi\Gamma)^{-1}\Pi\delta\boldsymbol{h}^0 \\ \delta\boldsymbol{Q} = \Pi\delta\boldsymbol{h}^0 + \sum_{n=1}^{\infty}(\Pi\Gamma)^n\Pi\delta\boldsymbol{h}^0 = \sum_{n=1}^{\infty}\delta\boldsymbol{Q}^{(n)} \end{gathered} \tag{20}$$

It formally requires the calculation of the inverse matrix of the order equal to the number of atoms in the TMC.

Though procedures of that sort are admitted in modern MM schemes directed to the systems with significant charge redistribution,[57] we consider such a procedure to be too resource consuming and restrict ourselves by several lower orders with respect to Π in the expansion. Then the term $\Pi\delta\boldsymbol{h}^0$ corresponds to the first order perturbation by the Coulomb field induced by the metal ion and bare (nonpolarized) ligand charges. The second order term corresponds to the perturbation due to the Coulomb field induced by the mutually polarized (upto the first order) charges

$$\begin{gathered} \delta\boldsymbol{Q}^{(1)} = \Pi\delta\boldsymbol{h}^0 \\ \delta\boldsymbol{Q}^{(2)} = \Pi\Gamma\Pi\delta\boldsymbol{h}^0 \end{gathered} \tag{21}$$

The atom−atom mutual polarizability matrix Π has a block-diagonal form

$$\Pi = \oplus_{\Lambda} \Pi^{\Lambda} \tag{22}$$

where Λ enumerates the ligands.

To evaluate Π^{Λ}, we consider the mutual atomic orbital polarizabilities $\Pi_{\alpha\beta}^{\Lambda(0)}$

$$\Pi_{\alpha\beta}^{\Lambda(0)} = \frac{\delta P_{\alpha\alpha}}{\delta h_{\beta\beta}} \tag{23}$$

where α and β enumerate AOs, and corresponding mutual atomic polarizabilities $\Pi_{AB}{}^{\Lambda(0)}$

$$\Pi_{AB}^{\Lambda(0)} = \frac{\delta Q_A}{\delta h_B} \tag{24}$$

where A and B enumerate atoms. Turning to the difference $\delta P_{\alpha\alpha}$ of the electron density on the αth AO of atom A and renormalizing $\delta h_{\beta\beta}$ accordingly to eq 19 results in

$$\delta P_{\alpha\alpha} = \sum_{B\neq A}\sum_{\beta\in B}\Pi_{\alpha\beta}^{\Lambda(0)}\delta h_{\beta\beta} = \sum_{B\neq A}\sum_{\beta\in B}\Pi_{\alpha\beta}^{\Lambda(0)}(\delta h_{\beta\beta}^{0} + \sum_{\mu}\tilde{\gamma}_{\alpha\mu}\delta P_{\mu\mu})$$

$$\delta \boldsymbol{Q} = \Pi^{\Lambda(0)}(\delta \boldsymbol{h}^{0} + \tilde{\gamma}\delta \boldsymbol{Q})$$

where $\tilde{\gamma}_{\alpha\mu}$ is the intraligand (Λ) two-electron Coulomb integral that in the CNDO approximation has the form

$$\tilde{\gamma}_{\alpha\beta} = (1 - \delta_{\alpha\beta})\gamma_{\alpha\beta} + \delta_{\alpha\beta}\gamma_{\alpha\alpha}/2 \tag{25}$$

The coefficient one-half at the diagonal interaction element in the above expression reflects the fact that in the single-determinant approximation with the closed shell only that half of electron density residing at the αth AO contributes to the energy shift at the same AO which corresponds to the opposite electron spin projection. Then the expression for the renormalized mutual atomic polarizability matrix Π^{Λ} can be obtained

$$\Pi^{\Lambda} = (1 - \tilde{\gamma}\Pi^{\Lambda(0)})^{-1}\Pi^{\Lambda(0)} \tag{26}$$

Finally, according to the general formulas given, say, in ref 56, the matrix element of the bare orbital mutual polarizability entering eq. 23 is given by

$$\Pi_{\alpha\beta}^{\Lambda(0)} = 4\sum_{k\in occ}\sum_{l\in vac}\frac{c_{l\alpha}c_{l\beta}c_{k\alpha}c_{k\beta}}{\epsilon_k - \epsilon_l}$$
$$\Pi_{AB}^{\Lambda(0)} = \sum_{a\in A}\sum_{\beta\in B}\Pi_{\alpha\beta}^{\Lambda(0)} \tag{27}$$

where α and β are the AOs indices, k and ϵ_k and l and ϵ_l are respectively the occupied and vacant MOs indices and orbital energies, and $c_{l\alpha}$ are the MO LCAO coefficients for the free molecule of the ligand Λ.

This is the method for construction the renormalized polarizability matrix Π^{Λ} for the ligand Λ. The form of the total matrix Π for the whole TMC is given by eq 22. With use of this matrix, we can obtain renormalized atomic charges by eq 20. This model can be termed here as the PS model (PS stands for perturbative sparkle). Specifically, the PSn approximation level of the PS model stands for the charge corrections of the series eq 20 up to the nth order, whereas PS itself stands for the exact expression with the inverse matrix in the second row of the same equation. Then, eqs 18−21 comprise the perturbative form of the sparkle model of the l system's electronic structure (the PS model).

Thus, in this subsection, we formulated the perturbative version of the sparkle approximation for the Green's function $\boldsymbol{G}_0^{\mathrm{l}}$ of the l system. It satisfies the requirement imposed above that the Green's function of the l system must be expressed in terms of those of the free ligands. As we show in section 4.2 below, it yields effective atomic charges of sufficient precision using the point charges of the free ligand as a zero approximation. The charges thus obtained are used for calculation of the $\Sigma_{ii}^{(f)}$ term according to eq 15 and for renormalizing the orbital energies by eq 14. The proposed procedure improves the junction between the EHCF(L) method playing the role of the QM procedure and the MM part, as shown below, where details of the calculations performed within this approximation are given (section 4).

3. Incorporating EHCF(L) into MM

3.1. Total Energy in the Hybrid EHCF(L)/MM Model. The total energy of a TMC in its nth electronic state in the EHCF(L)/MM approximation is taken as in ref 23 where it is shown to be

$$E_n = E_L + E_{\mathrm{d}}^{\mathrm{eff}}(n);\ E_{\mathrm{d}}^{\mathrm{eff}}(n) = \langle \Psi_n^{\mathrm{d}}|\ H_{\mathrm{d}}^{\mathrm{eff}}|\Psi_n^{\mathrm{d}}\rangle \tag{28}$$

where Ψ_n^{d} is the nth eigenfunction of the effective d shell Hamiltonian $H_{\mathrm{d}}^{\mathrm{eff}}$ eq 1 obtained from the full CI expansion of the d system wave function. Thus, the term $E_{\mathrm{d}}^{\mathrm{eff}}(n)$ is the d shell energy calculated as the nth eigenvalue of the effective d shell Hamiltonian. The ligand energy E_L is replaced by E_{MM}, the MM energy of the ligands. In the present work, we assume that the effective d shell Hamiltonian is estimated by the EHCF-(L) method described in the previous section. The contribution $E_{\mathrm{d}}^{\mathrm{eff}}(n)$ apparently is not a MM-like "force field" and has a different structure.

To obtain the effective Hamiltonian for the d shell used in eq 28 the electronic structure parameters (ESP's) of the l system must be used in eqs 1−4, 9, and 10. These ESP's are condensed in the l system Green's function. In the previous section, we presented general formulas which comprise the perturbation approach to evaluation of the Green's function of the l system using those of the separate free ligands as a zero approximation. Estimates of the l system Green's function following the prescriptions of section 2.1 can be performed for arbitrary molecular geometry. Inserting this approximate form of the l system Green's function into the EHCF(L) formulas, eqs 9 and 10 yield the required estimate for the crystal field acting on the d shell of a central TMI in terms of the separate increments of the lone pairs for each molecular configuration of the TMC.

The RLMO and PS models represent the Green's function G_0^{l} originated from eqs 11−13 including only the ligand MO energy shifts by $\Sigma_{ii}^{(f)}$ eq 15 calculated with use of the effective atomic charges. The latter are the charges for either free ligands or those polarized by metal ion and other ligands for the RLMO or PS models, respectively. That all comprises the two versions of the hybrid EHCF(L)/MM approach to evaluation of the PES of TMCs. The RLMO approach was thoroughly investigated in refs 39 and 40, so in the present paper, we focused on the PS model implementation.

3.2 Parameters Used in the EHCF(L)/MMGK Approach. The EHCF(L)/MMGK method described above in general terms is a specific case of a general hybrid scheme involving QM and MM components which both require extensive parametriza-

tion. The entire set of parameters consists of three subsets. In our case, these are the subsets related to the QM description of the d shell, the parameters of the MM part, and those relevant to the junction between the MM and QM subsystems.

3.2.1. d Shell Parameters. The d shell parameters are taken from the original EHCF method ref 43 without changes. These are the specific exponents of atomic d orbitals and d electron core attraction parameter U_{dd} for each metal atom. The Coulomb repulsion of d electrons is characterized by three parameters: g_{dd} and the Racah parameters B and C. In the general theoretical setting of the EHCF method, the Racah parameters must be taken standard for the free ions as tabulated, say, in ref 44. Pragmatically, however, the values specific for the complex are used in order to reach better agreement between theoretical and experimental spectra.[45−48] In the context of the present study directed toward uniform description of a wide range of complexes with many different ligands, only the single values of the Racah parameters common for all complexes of a given metal ion make sense. For the complexes of Fe (II), the Racah parameters $B_0 = 917$ cm^{-1} and $C_0 = 4040$ cm^{-1} for the free Fe^{2+} cation are used like in refs 43 and 47−49. In refs 45−48 where the EHCF method has been employed for electronic spectra calculations of some Co^{2+} complexes, various values of the Racah parameters have been used. For example, in the case of the complex $[CoCl_6]^{4-}$, these values were $B = 780$ cm^{-1} and $C = 3432$ cm^{-1},[47] whereas for the complexes $Co(H_2O)_6^{2+}$ and $[Co(NH_3)_6]^{2+}$ the values of $B = 850$ cm^{-1} and $C = 3935$ cm^{-1} and $B = 885$ cm^{-1} abnd $C = 4099$ cm^{-1} were used, respectively.[48] The free Co^{2+} ion Racah parameters are $B_0 = 971$ cm^{-1} and $C_0 = 4366$ cm^{-1}.[44] For the considered set of Co(II) complexes, the specific single set of these parameters for the Co^{2+} ion $B = 800$ cm^{-1} and $C = 3800$ cm^{-1} is used both for the low- and high-spin complexes with different coordination numbers and geometries. The employed Racah parameters are somewhat reduced as compared to the free ion values.

3.2.2. MM Parameters. The organic part of a molecule and metal ion coordination sphere (leaving out effects of the d shell) is described in the present hybrid procedure in terms of the MMGK method.[15,16]

Within it the total conformation energy of a molecule is

$$E_{MM} = \sum E_b + \sum E_{ang} + \sum E_{tors} + \sum E_{nb} + \sum E_{imp} + \sum E_{rep} \quad (29)$$

where the energy terms (force fields) are

$$E_b = \frac{1}{2}K_r(r - r_0)^2$$

the energy of bond stretching (except metal − donor atom bonds, see below)

$$E_{ang} = \frac{1}{2}K_\theta(\theta - \theta_0)^2$$

the energy of valence angle bending as in ref 1. The valence angles involving the metal ion as a vertex are not considered as they ar e described through the Gillespie-Kepert term[18] (see below eq 31)

$$E_{tors} = \frac{1}{2}V_0(1 + \cos[n(\phi + \psi)])$$

the energy of torsion interaction

$$E_{nb} = \epsilon_{ij}\left(\frac{r_0}{r_{ij}}\right)^{12} - 2\epsilon_{ij}\left(\frac{r_0}{r_{ij}}\right)^{6}$$

the energy of nonbonded interaction

$$E_{imp} = \frac{1}{2}K_{imp}\delta^2$$

the energy of improper torsion (out-of-plane) interaction.

Bonding interaction of metal valence 4s and 4p subshells with ligands is currently modeled within the MM part of the combined EHCF(L)/MM scheme through the Morse potential

$$E_b = D_0[e^{-\alpha(r-r_0)} - 1]^2 \quad (30)$$

The use of the Morse function is necessary to interpolate energy values in a wide range of variations of the metal−donor atom separations in different TMC spin states. It should be noted that our goal here is to employ a single parameter set for any spin state whereas in other approach used for the TMC structure calculations there are separate sets for the low- and high-spin states.[7]

The arrangement of the donor atoms around the metal is dictated by mutual repulsion between the effective centers lying on the M−L bonds on the distance r_{eff} from the metal ion. This term implicitly partially accounts for the electronic effects in the coordination sphere which could not be described within the standalone EHCF formalism (which gives only the d shell energy). The energy of the bond repulsion in the coordination sphere is then

$$E_{ij}^{rep} = A_iA_j/R_{ij}^{\ 6} \quad (31)$$

where

$$R_{ij}^{\ 2} = r_{i,eff}^{\ 2} + r_{j,eff}^{\ 2} - 2r_{i,eff}r_{j,eff}\cos(\widehat{X_iMX_j})$$

$$r_{i,eff} = R(M{-}X_i)d_{i,eff}$$

and $R(M-X_i)$ is the actual $M-X_i$ bond length; A_i, A_j, $d_{eff,i}$, and $d_{eff,j}$ are the GK force field parameters, characterizing energy of repulsion (A) and positions of the repulsion centers (d_{eff}).

The MM parameters for the organic part of the molecule were primarily taken from the CHARMM force field,[58,59] whereas specific metal-dependent parameters must be fitted within different versions of the EHCF(L)/MM method separately (compare ref 40 and the present work). We note once again that the single parameters set is used for all spin states of the TMI under consideration.

3.2.3. Junction Parameters. Since the EHCF(L)/MMGK approach is a specific case of a general QM/MM scheme, where the entire system is divided into two parts, namely the d shell and the l system, their interaction requires separate attention. Within the standard EHCF model, this interaction ultimately results in the d shell splitting. In the QM/MM context, the intersystem interacton is habitually termed as a junction. Not like in other hybrid QM/MM schemes, the form of the junction in the present EHCF(L)/MM scheme is not taken ad hoc but is given by the EHCF[43] and EHCF(L)[39,42] theories. The precise numerical values of the junction-related quantities are calculated on the basis of the theory reviewed above. An important component of this theory is that certain type of electronic structure underlying the MM part of the system is assumed. Parameters characterizing this implied electronic structure of the l system are used in order to estimate the intersystem

junction. These two kinds of parameters corresponding, respectively, to the d−l interaction itself and to the l system electronic structure (ESP's) are characterized below.

d−l Interaction Parameters. In the original EHCF theory, the specific parameters describing the interaction between the d and l systems were fit to reproduce the d level splitting for octahedral complexes with a specific donor atom. The set of the intersystem interaction parameters includes the g_{sd} and $\bar{g}_{pd}$ parameters of the Coulomb interaction between the d shell and transition metal valence s and p electrons. These parameters are taken from the Oleari's work,[60] the valence state ionization potentials for the d shell and the donor atoms are taken from ref 61, and the dimensionless factors β_{ML} characteristic for a metal−donor atom pair, scaling the resonance interaction. These parameters are transferred from the original EHCF[43] to the EHCF(L)/MM without change. The orbital exponents necessary for calculating the overlap integrals employed throughout the parametrizing the resonance integrals are also taken from ref 43 as they are there.

ESPs of the l System. RLMO Model. The ESPs of the l system required for the calculation of the effective Hamiltonian eq 1 are the one-electron densities (effective charges), orbital energies, and MO LCAO expansion coefficients. The original EHCF[43] method employs the CNDO approximation[53] in order to estimate these quantities. They are calculated for arbitrary molecular geometry by the approximate SCF procedure extended to the entire l system. The local version of the EHCF employed in the present work additionally requires a set of expansion coefficients for each local state (LMOs) related to the LP involved in the complex formation (located on the donor atoms), as parameters. The expansion coefficients of the LP over the donor atom AOs having the dominating contribution to the LP and calculated within the ligand fixed coordinate frame (LFCF) are treated as ESPs of the l system as well. These quantities proposed in ref 42 are calculated separately for the free ligand molecules and are fed to the EHCF(L)/MM procedure as parameters.

In the RLMO approximation of ref 39, the orbital energies are estimated perturbatively which is more economical from the computational point of view but requires a larger number of parameters. Within the RLMO model, the electronic structure of the free ligand prototype is supposed to be unchanged during the complex formation. Thus, for the EHCF(L) calculations, we use the charge distribution calculated for the free ligand itself, i.e., the effective point charges which are found from the CNDO calculation on the free ligand and consider them as ESPs for the l system. Also the orbital energies of the ligand MOs having nonzero contribution to the LP of the donor atom calculated for the free ligand are to be fed to the EHCF(L)/MM procedure. They are used to estimate the positions of the poles of the Green's function in the Coulomb field of the charges within the complex according to the formula eq 14 with use of the partial densities ρ_{iN} introduced above in eq 16 which are also considered as parameters. All these quantities are calculated separately with use of the CNDO parametrization for the free ligands.

ESPs of the l System. PS Model. The PS model of the electronic structure of the l system includes ESPs which are the same as in the RLMO model. The difference with the latter is that the effective charges used in eqs 19−21 are renormalized due to polarization by the Coulomb interaction between the ligands themselves and with the metal ion. By eq 22 the matrix of mutual atomic polarizabilities for the whole l system is constructed from the polarizability matrixes of the free ligands eq 26 calculated preliminary. All of the mutual polarizabilities between atoms of the different ligands are neglected since they have too small values. It was checked by direct test calculation of the entire polarizability matrix of separate ligands.

Then it is possible to calculate the polarized charges in all of the required orders by eq 21 starting from the bare ones. In fact, the second order in eq 21 and complete summation of the perturbation series by eq 20 give very close results. In most cases, the second or even the first-order polarization suffice for our purposes (see the next section).

TABLE 1: Parameters of the Morse and Gillespie−Kepert Potentials for the EHCF(L)-PS1/MMGK Model of the Ligand ESPs

metal ion	atom type	D_0, kcal/mol	α, $Å^{-1}$	r_0, Å	A, kcal $Å^6$/mol	d_{ff}
Fe^{2+}	NA	80.5	1.73	1.890	41.4	1
Fe^{2+}	N3	70.0	1.73	1.956	34.2	1
Co^{2+}	NA	110.0	1.20	1.86	44.8	1
Co^{2+}	N3	118.0	1.56	1.88	47.2	1

4. Results and Discussion

In our present study, the basic procedure for treating PES of TMC within a general QM/MM-like framework is constructed. To summarize, we reformulated in the local form (i.e., in terms of the effective field increments induced by the lone pairs of the ligands) the semiempirical EHCF theory which previously allowed us to calculate with quite good accuracy the crystal field induced by the ligands on the TMC's d shells. This gave us explicit formulas for the crystal field matrix expressed through the ESPs of the free ligands and the procedure to calculate them. In the framework of our approach, the crystal field matrix is calculated for arbitrary arrangement and orientation of the ligands around the central TMI.

4.1. Implementation. In the present work, we constructed a procedure combining the EHCF(L) approach and the specific form of the MM (MMGK ref 16) by eq 28. It is implemented within the ECFMM 1.1 package[54] which allows gradient minimization for the energy eq 28. The package also allows us to consider ligands or their fragments also as rigid bodies. As a consequence, the number of geometry variables considerably decreases which allows us to speed up the minimization. Technically, the ligand geometries employed within the rigid body scheme are first pre-optimized with use of the MM potentials only, and in the further calculations, their internal geometry is fixed. The PS1 and PS2 orders for charges as well as the exact PS calculation of the PS model are implemented in the ECFMM package. In our calculations, we used the PS1 model. Parameters fitted within the EHCF(L)-PS1/MMGK model for pairs metal atom−donor atom, where metal is Fe(II) or Co(II) and donor atom types (MMGK) are NA and N3, that is sp^2- and sp^3-hybridized nitrogen, are present in Table 1. Names and Cambridge Crystal Structure Data Bank (CCSDB) codes of the calculated complexes are listed in Table 2.

4.2. Numerical Simulation with Use of the PS Model. As it is stated in section 2.1, the effective charges and orbital energies of the l system are needed to estimate the EHCF. In the EHCF method of ref 43, these quantities are calculated with the use of the semiempirical SCF procedure (CNDO). We compared the free ligand charges and the charges calculated within the SCF sparkle estimates and PS estimates according to the procedure described in section 2.3.2. The results are presented in Table 3. Numeration of the ligand atoms can be found in Figure 6.

TABLE 2: Ligand Names and CCSD Reference Codes for the Calculated Molecules

no.	ligand name	ground state spin (exp.)	CCSD refcode	ref.
1	tris(2,2′-bipyridine)	0	NUZKOI	62
2	bis(tris(2-pyridyl)amine)	0	PYAMFE	63
3	bis(tris(2,2′-bipyrimidine)	0	RIJLAX	64
4	tris(5,5′,6,6′-tetramethyl-3,3′-bi-1,2,4-triazine)	0	HEYRAE	65
5	bis(2-(pyrazin-2-ylamino)−4-(pyridin-2-yl)thiazole)	0	RIZSOI	66
6	bis(2,2′:6′,6″-terpyridine)	0	ZIMBUS	67
7	exo-(6,13-diamino-6,13-dimethyl-1,4,8,11-tetra-azatetradecane)	0	PAZXAP	25
8	bis(1,4,7-triazacyclononane)	0	DETTOL	68
9	(1,4,7-tris(2-pyridylmethyl)−1,4,7-triazacyclononane)	0	DUCFOW	69
10	bis(2,2′-dipicolylamine-N,N′,N″)	0	JALJAH	70
11	hexapyridine	2	PYFEFE	71
12	tris(6-methyl-2,2′-bipyridine-N,N′)	2	VEWVEY	72
13	hexakis(1-methylimidazole)	2	MIMFEA	73
14	hexakis(isoxazole-N)	2	QAHPIY	74
15	tris(2,2′-bibenzimidazole)	2	VEYTEY	75
16	tris(2,2′-bi-imidazole-N,N′)	2	ZIMMAJ	76
17	tris(2-(1,5-dimethyltriazol-3-yl)pyridine)	2	YIVSEB	77
18	bis(tris(3,5-dimethyl-1-pyrazolyl)methane-N,N′,N″)	2	XEFDER	78
19	delta-(1,4,7-tris(2-aminophenyl)−1,4,7-triazacyclononane)	2	LOTSES	79
20	tris(ethylenediamine)	2	ZIWDUG	80
21	bis(bis(1-methylimidazol-2-ylmethyl)amine-N,N′,N″)	2	NARWIM	81
22	bis(tris(2-pyridylmethyl)amine-N,N′,N″)	2	NELGIU	82
23	bis(4,6-diphenyl-2,2′:6′,2″-terpyridine)	2	JOJQEE	84
24		0	JOJMUQ	84
25	bis(2,6-bis(pyrazol-1-yl)pyridine)	2	XENBEX01	85
26		0	XENBEX03	85
27	tris(3-(pyridin-2-yl)−1,2,4-triazole-N,N′)	2	QALMAR	86
28		0	QALMAR01	86
29	tetrakis(2-pyridylmethyl)ethylenediamine	2	KEZPEK	87
30		0	KEZPIO01	87
31	tris(2,2′-bipyridine)	3/2	CAMHED	88
32	bis(2,2′:6′,6″-terpyridine)	3/2	CAPSAN	89
33	hexakis-imidazole	3/2	ROJXET	90
34	tetrakis(1,2-dimethylimidazole-N^3)	3/2	FUJHAT	91
35	(4,14,19-tris(methoxymethyl)-1,4,6,9,12,14,19,21-octa-azabicyclo(7.7.7)tricosane)	3/2	NEBLIP	92
36	1,4,8,11-tetra-azacyclotetradecane	1/2	COANEC	93
37	aqua-12,14-dimethyl-1,4,8,11-tetra-azacyclotetradeca-11,13-diene	1/2	MTZCOF	94
38	(3-(1-(methylamino)ethylidene)−11-(1-(methylimino)ethyl)-2,12-dimethyl-1,5,9,13-tetra-azacyclohexadeca-1,4,9,12-tetraene-N)	1/2	FAZPUR	96
39	aqua-5,7,7,12,14,14-hexamethyl-1,4,8,11-tetra-azacyclotetradeca-4,11-diene	1/2	JASKUJ	95
40	(5,7,12,14-tetramethyl-2,3:9,10-dibenzo-1,4,8,11-tetra-aza(14)annulene)	1/2	JUHTIP	97

The data of Table 3 show that the free ligand effective atomic charges (column 1) are quite strongly affected by the interaction with metal ion described by the SCF sparkle procedure (column 2). The difference between the results of the SCF sparkle model (column 2) and the charges obtained by the PS1 model (column 3) is however small especially for charges of the peripheral atoms. Charges on the donor atoms in column 3 are slightly larger than these in column 2, but the difference is also small. On the other hand, the difference between SCF sparkle (column 2) and free ligand (column 1) charges are close to the difference between columns 3 and 1. One can see that whatever method of taking into account the charge renormalization gives rather close results when it goes about the charges on all the ligand atoms except the donor ones. However, 90% of the d level splitting comes from the covalent contribution eq 5 so even large error in the donor atom charges does not destroy the overall estimate of the effective crystal field.

The values of the orbital energies are obtained from eq 15 that is the first-order correction to the orbital energy for the MO in the field induced by all of the charges of the complex except those in the ligand under consideration itself. The charges in eq 15 are taken from the PS1 model. Orbital energies are close to those obtained within the sparkle SCF scheme (see Table 4). Thus, such an approximation for the orbital energies of the ligands is shown to simulate the results of the SCF sparkle model.

In conclusion, the first-order polarized point charges as well as the orbital energies eq 15 using these charges of eq 21 are found to be in fair agreement with those from a semiempirical SCF procedure corresponding to the sparkle model.

4.3. EHCF(L)-PS1/MMGK Model. *4.3.1. Spin States and Geometry of Iron(II) Complexes.* The methodology described above was applied to 30 complexes of Fe^{2+} listed in Table 2 together with the ligand names, relevant Cambridge Crystal Structure Data Bank (CCSDB) reference codes, and the experimental spins of the ground states. The ligands are shown in Figure 6. The series contains compounds with monodentate and polydentate ligands of both low- and high-spin ground states.

Experimental geometries of the above complexes were taken from the CCSDB. Hydrogen atoms were added where necessary. For complexes 23−30 that exhibit spin-crossover, crystal structures for both low- and high-spin states are known which allows for a detailed comparison of the results of our calculations with experiment (at least in terms of molecular geometry).

As a test, we calculated the 10*Dq* parameter for octahedral complex 11 as a function of the metal−nitrogen distance with use of the EHCF(L)-PS1 and by the original EHCF procedure. It was found that for the "interesting" range of the interatomic separations (about 2 Å) either first or second perturbation orders of the EHCF(L)-PS1 model employed in the present work fairly

TABLE 3: Comparison of Effective Charges on the Ligands Obtained by Different Models

atom	free ligand (1)	sparkle SCF (2)	EHCF(L) PS1 (3)	δQ (2)−(1)	δQ (3)−(1)	δQ (3)−(2)
			Bipyridine in **1**			
N	−0.157	−0.412	−0.370	−0.255	−0.213	0.042
C(1)	0.095	0.121	0.084	0.026	−0.011	−0.037
C(2)	0.081	0.140	0.130	0.059	0.049	−0.010
C(3)	−0.030	−0.014	−0.020	0.016	0.010	−0.006
C(4)	0.035	0.083	0.070	0.048	0.035	−0.013
C(5)	−0.035	−0.017	−0.010	0.018	0.025	0.007
			Terpyridine in **6**			
N(1)	−0.150	−0.403	−0.389	−0.253	−0.239	0.014
N(2)	−0.158	−0.448	−0.432	−0.290	−0.274	0.016
C(1)	0.098	0.115	0.122	0.017	0.024	0.007
C(2)	0.087	0.143	0.139	0.056	0.052	−0.004
C(3)	−0.028	−0.014	−0.018	0.014	0.010	−0.004
C(4)	0.032	0.082	0.070	0.050	0.038	−0.012
C(5)	−0.035	−0.014	−0.018	0.021	0.017	−0.004
C(6)	0.098	0.137	0.137	0.039	0.039	0.000
C(7)	−0.035	−0.020	−0.020	0.015	0.015	0.000
C(8)	0.031	0.083	0.071	0.052	0.040	−0.012
			Pyridine in **11**			
N	−0.149	−0.373	−0.348	−0.224	−0.199	0.025
C(1)	0.090	0.116	0.134	0.026	0.044	0.018
C(2)	−0.015	−0.005	−0.010	0.010	0.005	−0.005
C(3)	0.041	0.079	0.077	0.038	0.036	−0.002
			Methyl-bipyridine in **12**			
N(1)	−0.147	−0.375	−0.323	−0.228	−0.176	0.052
N(2)	−0.177	−0.407	−0.341	−0.230	−0.164	0.066
C(1)	0.102	0.112	0.125	0.010	0.023	0.013
C(2)	0.107	0.127	0.136	0.020	0.029	0.009
C(3)	−0.031	−0.012	−0.017	0.019	0.014	−0.005
C(4)	0.051	0.077	0.080	0.026	0.029	0.003
C(5)	−0.046	−0.017	−0.033	0.029	0.013	−0.016
C(6)	0.101	0.118	0.096	0.017	−0.005	−0.022
C(7)	0.128	0.161	0.129	0.033	0.001	−0.032
C(8)	−0.042	−0.030	0.073	0.012	0.115	0.103
C(9)	0.048	0.082	0.101	0.034	0.053	0.019
C(10)	−0.039	−0.027	0.043	0.012	0.082	0.070
C(11)	0.009	−0.069	−0.064	−0.078	−0.073	0.005
			Ethylenediamine in **20**			
N(1)	−0.236	−0.436	−0.416	−0.200	−0.180	0.020
C(1)	0.080	0.067	0.068	−0.013	−0.012	0.001
N(2)	−0.234	−0.429	−0.412	−0.195	−0.178	0.017
C(2)	0.084	0.070	0.067	−0.014	−0.017	−0.003

TABLE 4: Comparison of Orbital Energies (a.u.) of the Ligands Obtained by Different Models

MO number	free ligand	sparkle SCF	EHCF(L) PS1
	Bipyridine in **1**		
1	−1.9351	−2.2389	−2.2198
6	−1.3104	−1.5962	−1.5578
14	−0.8627	−1.1505	−1.1475
23	−0.5522	−0.8385	−0.7965
28 (HOMO)	−0.4563	−0.7593	−0.7223
	Pyridine in **11**		
1	−1.8319	−2.0728	−2.0683
2	−1.3946	−1.6510	−1.6447
4	−1.1013	−1.3178	−1.3152
6	−1.0037	−1.2336	−1.2295
9	−0.7026	−0.9566	−0.9524
11	−0.6526	−0.8776	−0.8745
15 (HOMO)	−0.4826	−0.7188	−0.7146

coincide with the standard EHCF curve which for the purposes of the present paper is considered as the exact one. Thus, it is not necessary to use the renormalized Racah parameters, which we used in refs 39 and 40. So, unlike the RLMO model,[40] we are able to use a single parameter set on the metal d shell for ligands containing both the NA (sp^2) and N3 (sp^3) nitrogen atom types.

Parametrizations for the NA and N3 atom types were performed separately. The proposed EHCF(L)-PS1 method was initially applied to a test set of the Fe^{2+} complexes. The test set comprised complexes 1, 2, 12, and 13 (for NA) and 7, 19, and 20 (for N3). Structures of the test set with different spin states (singlet and quintet) were optimized by an analytical gradient procedure starting from the experimental structures with rigid (preliminary optimized with pure MMGK) ligands. Optimization is performed until root-mean-squared (RMS) energy gradient is smaller than 0.1 kcal mol^{-1} $Å^{-1}$. Criteria for good parametrization are the correct ground spin state and small difference in molecular geometry of coordination sphere (bond lengths and valence angles on metal atom). Obtained parameters are presented in Table 1. One can see that the rigidity of the metal−ligand bond, measured by $D_0\alpha^2$ for the N3 type atom parameter, is only slightly smaller than that for the NA type atom. Geometry optimization for the rest of the series of the investigated complexes was performed by the same scheme but with the use of the parameters already defined.

Below we consider the results of our calculations of Fe(II) complexes of Table 2. The possible terms or spin states considered in calculations are quintet ($^5T_{2g}$) and singlet ($^1A_{1g}$) prototypes for approximately octahedral coordination of the Fe^{2+} ion. For visualization, we put the inverse empirical distribution function for root-mean-squared differences (RMSD), separately for high- and low-state molecules and for the whole data set (Figures 2−4), in the normal scale together with its linear fit to test whether our results may deviate systematically from experimental data. In general, plot of the empirical distribution function (error function) is a good statistical test on systematic error in the calculations. It characterizes both the range of observed errors and the possibility to meet them in our sample. It is supposed that the random errors are normally distributed with zero dispersion. Thus, it is clear from the linear fit plots in Figures 2−4 that systematic error is small for the whole data set, whereas for the separate low- and high-spin sets, they are larger. It can be seen also that for the low-spin complexes the Fe−N bond lengths are on the average somewhat too long, whereas for the high-spin ones, these lengths are somewhat too short. By linear fit, we also obtained the most probable value for RMSD, that is, the inverse coefficient of the linear fit. Thus, the geometry of both low- and high-spin molecules is calculated with the RMSD for the Fe−N bond lengths to be about 0.05 Å. If only the low-spin molecules are considered then RMSD is 0.034 Å, whereas for the high-spin molecules, only the RMSD is about 0.05 Å.

The detailed results of calculations can be found in Tables 5 and 6 of the Supporting Information, where calculated metal−donor atom bond lengths and averaged valence angles centered on metal atom are given for different spin states of the metal together with corresponding experimental crystal structure values.

Calculated geometries of this series of the complexes, in general, agree rather well with the experimental data. We especially notice that complexes with ligands containing different types of donor atoms (NA and N3) in the single molecule are calculated correctly. However, making parametrization, we should keep in mind that the crystal structure can be a result of not only metal interaction with the ligands but also of intermolecular interactions among the crystal neighbors. Thus, major deviations from the experimental geometry may be a

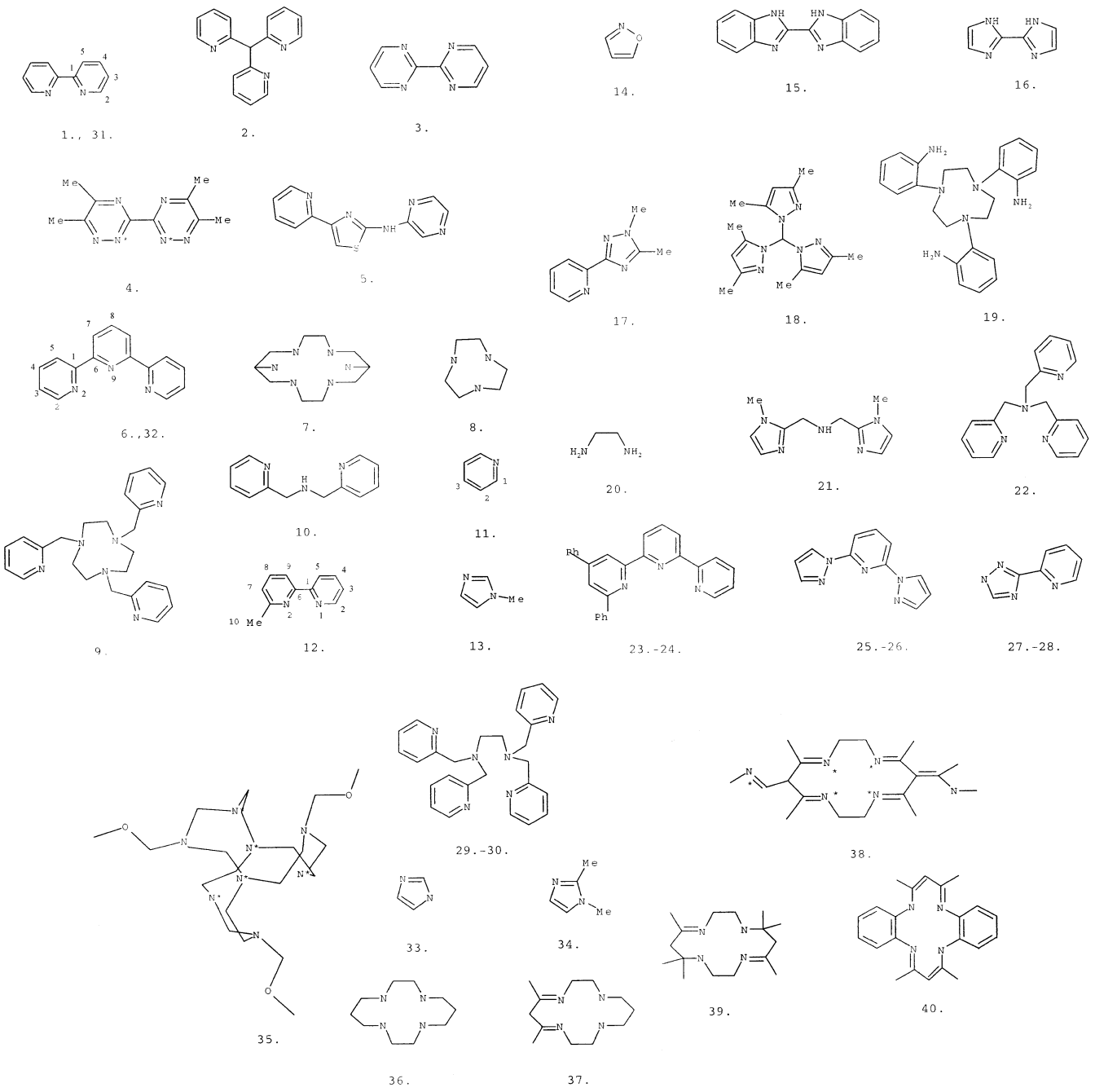

Figure 1. Ligands used in calculations. Donor atoms are marked explicitly (*).

result of crystal surrounding influence, especially that of counterions (see discussion in ref 40). Statistical analysis of obtained results performed above shows that geometry structure details are in good agreement with crystal data. However, in complexes 4−6 with low-spin experimental structure, our method gives the wrong ground-spin state but the correct geometry for the experimental low-spin state. For the high-spin complexes 11−22 as well as for the low-spin complexes 1−3 and 7−10, we obtain both the correct ground spin state and acceptable geometry. It can be concluded that current parametrization of the EHCF(L)-PS1 method is somewhat biased toward the high-spin states. This manifests itself in the fact that the calculated high-spin state equilibrium geometries correspond to noticeably shorter Fe−N bond lengths than the experimental ones. Technically, the reason may be the stiffness of the Morse potential employed to model the Fe−N bonding MM energy increment. For the complexes with spin isomers, we obtained similar result, since in all of the cases the high-spin form of the isolated molecular metal containing complex cations have lower energy. Analysis of effects of counteranions upon the spin forms in the spin-crossover compounds is given in ref 40.

We checked also the energy splitting between ground states and excited states of different symmetry and spin in the studied complexes and found that these states are considerably separated in energy (at least, by ≈20 kcal/mol).

To conclude, we notice that it is the first time when a calculation is performed for such a wide range of Fe(II) complexes (27 individual molecules) of different ground state spins within single parametrization and reproduces ground state spin as well as the geometry of the crystal structure with reasonable accuracy. However, it is still hardly possible to compare our results with any other semiempirical methods, because, the authors were not in a position to find any pure

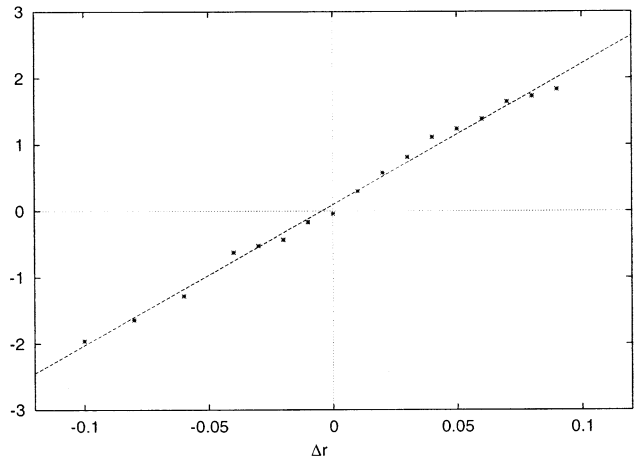

Figure 2. Empirical distribution function for RMSD bond lengths of both high- and low-spin Fe(II) complexes in the normal scale.

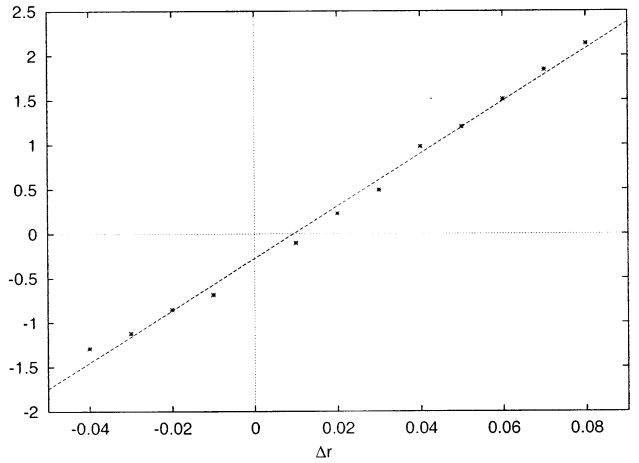

Figure 3. Empirical distribution function for RMSD bond lengths of low-spin Fe(II) complexes in the normal scale.

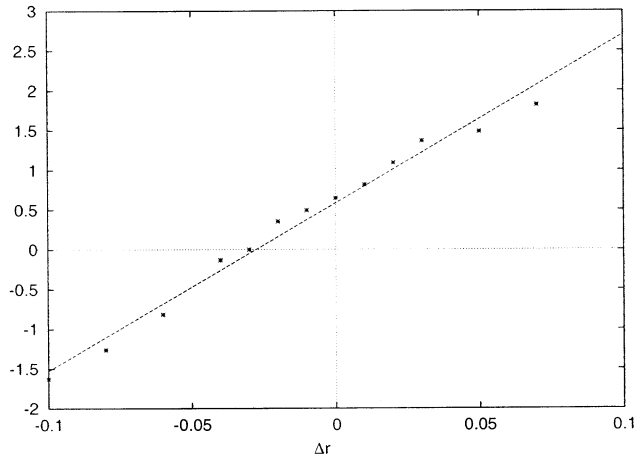

Figure 4. Empirical distribution function for RMSD bond lengths of high-spin Fe(II) complexes in the normal scale.

semiempirical method which would be able even to calculate the series of complexes we considered.

4.3.2. Spin States and Geometry of Cobalt(II) Complexes. Within the proposed version of the EHCF(L) method, we also calculated a series of Co^{2+} complexes with different shapes of coordination polyhedra. For an illustrative presentation of the results, we also constructed the empirical distribution function in normal scale together with its linear fit, as we did for Fe(II) complexes, separately for high- and low-state molecules and

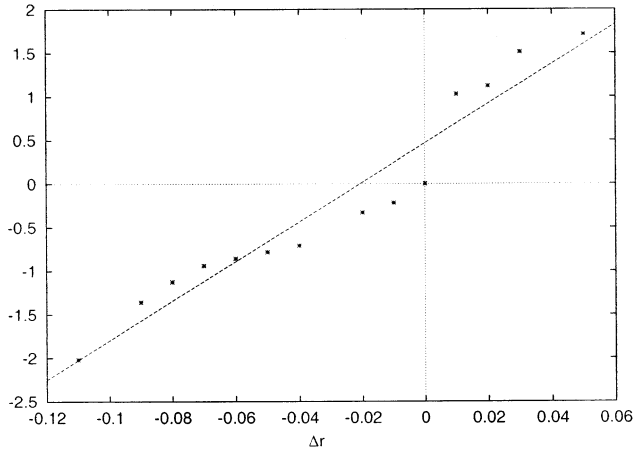

Figure 5. Empirical distribution function for RMSD bond lengths of both high- and low-spin Co(II) complexes in the normal scale.

for the whole data set (Figures 5−7). The detailed results of calculations can be seen in Table 7 of the Supporting Information.

We tried to have maximal diverse test calculation. Thus, we selected octahedral 31−33, tetrahedral 34, and pyramidal 35 high-spin (quartet with the prototype state $^4T_{1g}$) complexes, the low-spin square pyramidal 38 complex, and square planar complexes 36−37 and 39−40 (doublet with the prototype state $^2T_{1g}$). The entire set of the Co^{2+} complexes was used for parametrization of the NA and N3 atom types. With use of the Racah parameters $B = 800$ cm^{-1} and $C = 3800$ cm^{-1}, the ground spin states are reproduced for the whole set of the compexes calculated at their experimental geometries. This parametrization allows us to obtain even more precise results than those for the Fe^{2+} complexes with the RMSD = 0.044 Å for the bond lengths of the whole data set.

In the high-spin complexes 31−35, the structure and spin states are correctly predicted with RMSD = 0.054 Å for Co−N bond lengths (Figure 6). Interestingly, complex 32 is known to be near the spin crossover point in the solution.[98] According to our calculations, the energy difference between quartet and doublet minima for this complex is the smallest among all of the complexes 31−35 and is equal to 3.7 kcal/mol, whereas in other cases, it is more than 10 kcal/mol (see Table 7 of the Supporting Information).

Remarkably enough that the same parametrization allows us to reproduce the ground-state spin for the low-spin compounds 36−40 provided the calculation is performed with due caution. Particularly, in complexes 37 and 39, we have to include in the molecule a water ligand lying above the square plane by 2.21 Å and 2.28 Å correspondingly, taken from the experimental crystal structure of the complexes, for correct calculation of the crystal field. Its position was fixed during the optimization procedure. On the contrary, the unit cell of the complex 36 contains two ClO_4^- counterions which were considered in ref 93 as extremely weakly bonded (the bond distance Co−O(ClO_4^-) is 2.409 Å). We optimize the ion complex 36 itself and that including two ClO_4^- anions fixed at their positions taken from the experimental unit cell. By our calculation, the optimized geometry and spin of the ground state for the molecule 36 and that with counteranions are entirely the same. For the low-spin complexes 36−40, the average RMSD for the Co−N bond lengths is 0.036 Å (Figure 7), so for the square

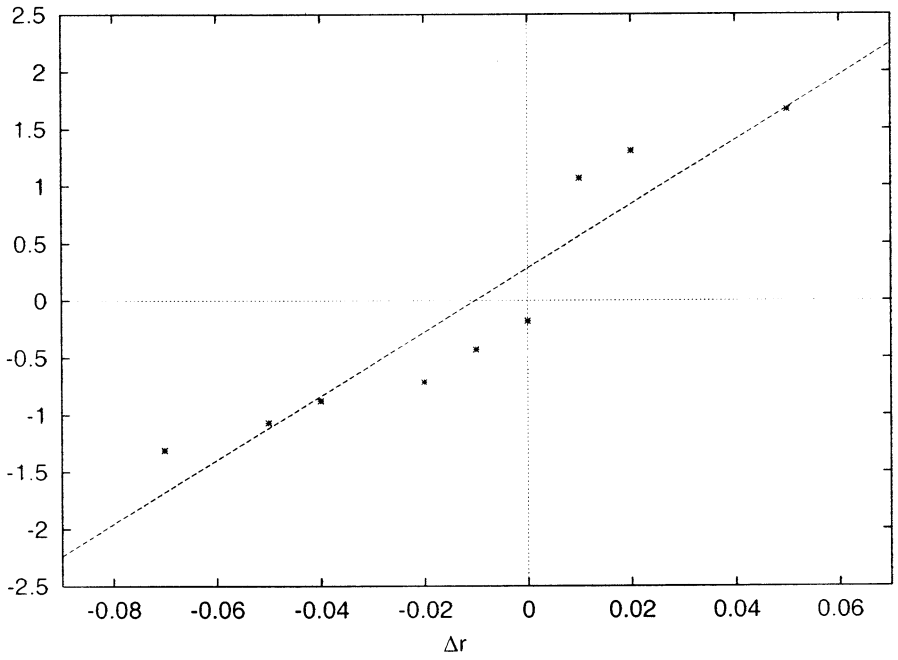

Figure 6. Empirical distribution function for RMSD bond lengths of low-spin Co(II) complexes in the normal scale.

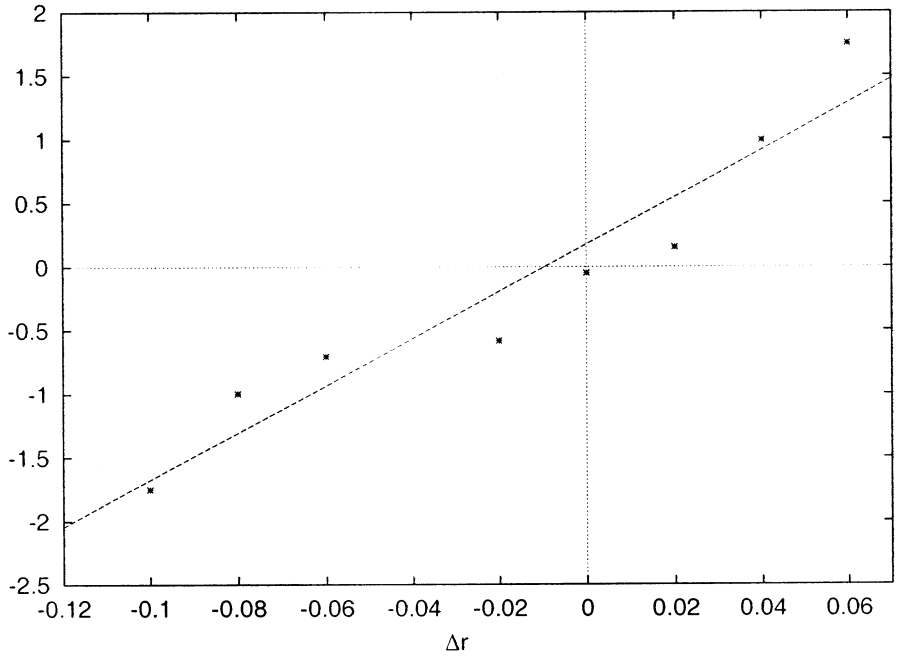

Figure 7. Empirical distribution function for RMSD bond lengths of high-spin Co(II) complexes in the normal scale.

pyramidal 38 and the square planar 40, the geometry was also correctly predicted.

The results show that the proposed method can be used for precise calculation on geometry and spin states of Co^{2+} complexes with different coordination numbers and coordination patterns. The proposed methodology thus covers in a uniform way different ground-state spins and even coordination numbers of the cobalt(II) complexes.

5. Conclusion

On the basis of the above analysis, it can be stated that the concert usage of the EHCF(L)-PS1 procedure as a QM component for describing the geometry dependence of the d shell energy together with the MMGK procedure as the MM component for describing the ligand energy, a unified QM/MM-like description for the PES of different spin states of the iron(II) and cobalt(II) complexes with nitrogen-containing ligands is achieved with use of the single spin-independent parametrization specific for each metal atom and MM type of the donor atom.

The used EHCF(L) procedure allows for a detailed description of the d shell energy as a function of composition and geometry of the ligand sphere, taking into account the correlation of electrons in the d shell by using the full CI wave function for them. This allows us to handle correctly the reaction of the d shell to subtle changes of the crystal field induced by the surrounding and by this to be sure that the spin intersection point is correctly located. The proposed method originated from the EHCF theory and can be also applied to the description of the low-lying excited states of certain TMCs.

On the other hand, due attention is paid to reproducing the dependence of the crystal field itself on the tiny ligand geometry and ESPs variations. The explicit forms for the crystal field matrix elements reproduce their dependence not only on interatomic separations but also on all kinds of valence angles.

Acknowledgment. The authors gratefully acknowledge Dr. I. V. Pletnev for valuable discussions and providing the wrapping MMGK suite MMPC 1030.[16] The authors are grateful to Profs. T.W. Hambley and M. Zimmer for sending reprints of their recent works. The authors are thankful to Referees for their valuable remarks and suggestions. The usage of the CCSDB is supported by the RFBR Grant No. 99-07-90133. This work has been supported by the RAS through Grant No. 6-120 dispatched by the Young Researchers Commission of RAS, and by the RFBR Grant Nos. 02-03-32087, 04-03-32146, and 04-03-32206.

Supporting Information Available: Detailed results of calculations in Tables 5−7. This material is available free of charge via the Internet at http://pubs.acs.org.

References and Notes

(1) Burkert, U.; Allinger, T. *Molecular Mechanics*; ACS: Washington, DC, 1982.
(2) Hay, B. P. Coord. *Chem. Rev.* **1993**, *126*, 177.
(3) Rappé, A. K.; Colwell, K. S.; Casewit, C. J. *Inorg. Chem.* **1993**, *32*, 3438.
(4) Landis, C. R.; Cleveland, T.; Firman, T. K. *J. Am. Chem. Soc.* **1995**, *117*, 1859.
(5) Landis, C. R.; Firman, T. K.; Root, D. M.; Cleveland, T. *J. Am. Chem. Soc.* **1998**, *120*, 1842.
(6) Comba, P.; Hambley, T. W. *Molecular Modelling of Inorganic Compounds*; VCH: Weinheim, Germany, 1995.
(7) Comba, P. *Coord. Chem. Rev.* **1999**, *182*, 343.
(8) Lehmann, T. J. *Biol. Inorg. Chem.* **2002**, *7*, 305.
(9) Sabolović, J.; Tautermann, C. S.; Loerting, T.; Liedl, K. R. *Inorg. Chem.* **2003**, *42*, 2368.
(10) Hambley, T. W.; Jones, A. R. *Coord. Chem. Rev.* **2001**, *212*, 35.
(11) Zimmer, M. *Coord. Chem. Rev.* **2001**, *212*, 133.
(12) Gütlich, P.; Garcia, Y.; Goodwin, H. A. *Chem. Soc. Rev.* **2000**, *29*, 419.
(13) Reichert, D. E.; Hancock, R. D.; Welch, M. J. *Inorg. Chem.* **1996**, *35*, 7013.
(14) Cundari, T. R.; Fu, W.; Moody, E. W.; Slavin, L. L.; Snyder, L. A.; Sommerer, S. O. *J. Phys. Chem.* **1996**, *100*, 18057.
(15) Pletnev, I. V.; Melnikov, V. L. *Koord. Khim.* **1997**, *23*, 205 [in Russian].
(16) Razumov, M. G.; Melnikov, V. L.; Pletnev, I. V. J. *Comput. Chem.* **2001**, *22*, 38.
(17) Gillespie, R. J.; Hargittai, I. *The VSEPR Model of Molecular Geometry*; Allyn and Bacon: Boston, MA, 1991.
(18) Kepert, D. L. *Inorganic Stereochemistry*; Springer: Berlin, 1982.
(19) Burton, V.; Deeth, R.; Kemp, C.; Gilbert, P. *J. Am. Chem. Soc.* **1995**, *117*, 7.
(20) Darkhovskii, M. B. *M.Sc. Thesis*, 1996.
(21) Tchougréeff, A. L. In *Molecular Modeling and Dynamics of Bioinorganic Systems*; Banci, L., Comba, P., Eds.; NATO ASI workshop; Kluwer: Dordrecht, The Nethelands, 1997; p 217.
(22) Deeth, R.; Paget, V. J. *Chem. Soc., Dalton Trans.* **1997**, 537.
(23) Darhovskii, M. B.; Tchougréeff, A. L. *Chem. Phys. Reps.* **1999**, *18*, 73.
(24) Comba, P.; Hambley, T. W.; Hitchman, M. A.; Stratemeier, H. *Inorg. Chem.* **1995**, *34*, 3903.
(25) Börzel, H.; Comba, P.; Pritzkow, H.; Sickmüller, A. *Inorg. Chem.* **1998**, *37*, 3853.
(26) Bersuker, I. B.; Leong, M.; Boggs, J.; Pearlman, R. *Int. J. Quantum Chem.* **1997**, *63*, 1051.
(27) Cini, R.; Musaev, D. G.; Marzilli, L. G.; Morokuma, K. *J. Mol. Struct. (THEOCHEM)* **1997**, *392*, 55.
(28) Maseras, F. *Chem. Commun.* **2000**, 1821.
(29) Comba, P.; Lledós, A.; Maseras, F.; Remenyi, R. *Inorg. Chem. Acta* **2001**, *324*, 21.
(30) Dewar, M. J. S.; Jie, C.; Yu, J. *Tetrahedron* **1993**, *49*, 5003.
(31) Thiel, W.; Voityuk, A. A. *J. Phys. Chem.* **1996**, *100*, 616.
(32) Cundari, T. R.; Deng, J. *J. Chem. Inf. Comput. Sci.* **1999**, *39*, 376.
(33) Pudzianowski, A. T. *Int. J. Quantum Chem.* **2002**, *88*, 147.
(34) Adam, K. R.; Atkinson, I. M.; Lindoy, L. F. *J. Mol. Struct.* **1996**, *384*, 183.
(35) Margulis, C. J.; Guallar, V.; Sim, E.; Friesner, R. A.; Berne, B. J. *J. Phys. Chem. B* **2002**, *106*, 8038.
(36) Landis, C. R.; Cleveland, T.; Firman, T. K. *J. Am. Chem. Soc.* **1998**, *120*, 2641.
(37) Firman, T. K.; Landis, C. R. *J. Am. Chem. Soc.* **1998**, *120*, 12650.
(38) Firman, T. K.; Landis, C. R. *J. Am. Chem. Soc.* **2001**, *123*, 11728.
(39) Darhovskii, M. B.; Razumov, M. G.; Pletnev, I. V.; Tchougréeff, A. L. *Int. J. Quantum Chem.* **2002**, *88*, 588.
(40) Darkhovskii, M. B.; Pletnev, I. V.; Tchougréeff, A. L. *J. Comput. Chem.* **2003**, *24*, 1715.
(41) Tchougréeff, A. L. *Phys. Chem. Chem. Phys.* **1999**, *1*, 1051.
(42) Darhovskii, M. B.; Tchougréeff, A. L. Russ. *J. Phys. Chem.* **2000**, *75*, 112.
(43) Soudackov, A. V.; Tchougréeff, A. L.; Misurkin, I. A. *Theor. Chim. Acta* **1992**, *83*, 389.
(44) Lever, A. B. P. *Inorganic Electronic Spectroscopy*; Elsevier Science: Amsterdam, 1984.
(45) Soudackov, A. V.; Tchougréeff, A. L.; Misurkin, I. A. *Int. J. Quantum Chem.* **1996**, *57*, 663.
(46) Soudackov, A. V.; Tchougréeff, A. L.; Misurkin, I. A. *Int. J. Quantum Chem.* **1996**, *58*, 161.
(47) Soudackov, A. V.; Tchougréeff, A. L.; Misurkin, I. A. *Russ. J. Phys. Chem.* **1994**, *68*, 1256.
(48) Soudackov, A. V.; Tchougréeff, A. L.; Misurkin, I. A. *Russ. J. Phys. Chem.* **1994**, *68*, 1264.
(49) Tchougréeff, A. L.; Soudackov, A. V.; Misurkin, I. A.; Bolvin, H.; Kahn, O. *Chem. Phys.* **1995**, *193*, 19.
(50) Perkins, P. G.; Stewart, J. J. P. *J. Chem. Soc., Faraday Trans. 2* **1982**, *78*, 285.
(51) Gerloch, M.; Wooley, R. G. *Struct. Bond.* **1983**, 371.
(52) Abrikosov, A. A.; Gor'kov, L. P.; Dzyaloshinskii, I. E. *Methods of Quantum Field Theory in Statistical Physics*, 2nd ed.; Dobrosvet: Moscow, 1998 [in Russian].
(53) Pople, J. A.; Beveridge, D. L. *Approximate Molecular Orbital Theory*; McGraw-Hill: New York, 1970.
(54) http://qcc.ru/~ netlab: Entry ECFMM.
(55) de Andrade A. V. M.; da Costa, N. B., Jr.; Simas, A. M., de Sá G. F. *Chem. Phys. Lett.* **1994**, *227*, 349.
(56) Peacock, T. E. *Electronic Properties of Aromatic and Heterocyclic Molecules*; Academic Press: New York, 1965.
(57) Kozelka, J.; Archer, S.; Petsko, G. A.; Lippard, S. J. *Biopolymers* **1987**, *26*, 1245.
(58) Brooks, B. R.; Bruccoleri, R. E.; Olafson, B. D.; Dates, D. J.; Swaminathan, S.; Karplus, M. *J. Comput. Chem.* **1983**, *4*, 187.
(59) Smith, J. C.; Karplus, M. *J. Am. Chem. Soc.* **1992**, *114*, 801.
(60) Di Sipio, L.; Tondello, E.; De Michelis, G.; Oleari, L. *Chem. Phys. Lett.* **1971**, *11*, 287.
(61) Böhm, M. C.; Gleiter, R. *Theor. Chim. Acta* **1981**, *59*, 127.
(62) Dick, S. Z. *Kristallogr. New Cryst. Struct.* **1998**, *213*, 356.
(63) Kucharski, E. S.; McWhinnie, W. R.; White, A. H. *Aust. J. Chem.* **1978**, *31*, 53.
(64) De Munno, G.; Poerio, T.; Viau, G.; Julve, M.; Lloret, F. *Angew. Chem. Int. Ed. Engl.* **1997**, *36*, 1459.
(65) Breu, J.; Range, K.-J.; Herdtweck, E. *Monatsh. Chem.* **1994**, *125*, 119.
(66) Childs, B. J.; Cadogan, J. M.; Craig, D. C.; Scudder, M. L.; Goodwin, H. A. *Aust. J. Chem.* **1997**, *50*, 129.
(67) Laine, P.; Gourdon, A.; Launay, J.-P. *Inorg. Chem.* **1995**, *34*, 5156.
(68) Boeyens, J. C. A.; Forbes, J. C. A.; Hancock, R. D.; Wieghardt, K. *Inorg. Chem.* **1985**, *24*, 2926.
(69) Christiansen, L.; Hendrickson, D. N.; Toftlund, H.; Wilson, S. R.; Xie, C.-L. *Inorg. Chem.* **1986**, *25*, 2813.
(70) Butcher, R. J.; Addison, A. W. *Inorg. Chim. Acta* **1989**, *158*, 211.
(71) Doedens, R. J.; Dahl, L. F. *J. Am. Chem. Soc.* **1966**, *88*, 4847.
(72) Onggo, D.; Hook, J. M.; Rae, A. D.; Goodwin, H. A. *Inorg. Chim. Acta* **1990**, *173*, 19.
(73) Seel, F.; Lehnert, R.; Bill, E.; Trautwein, A. Z. *Naturforsch., Teil B* **1980**, *35*, 631.
(74) Hibbs, W.; Arif, A. M.; van Koningsbruggen, P. J.; Miller, J. S. *CrystEngComm* 1999, *4*.
(75) Boinnard, D.; Cassoux, P.; Petrouleas, V.; Savariault, J.-M.; Tuchagues, J.-P. *Inorg. Chem.* **1990**, *29*, 4114.
(76) Lorente, M. A. M.; Dahan, F.; Sanakis, Y.; Petrouleas, V.; Bousseksou, A.; Tuchagues, J.-P. *Inorg. Chem.* **1995**, *34*, 5346.
(77) Sugiyarto, K. H.; Craig, D. C.; Rae, A. D.; Goodwin, H. A. *Aust. J. Chem.* **1995**, *48*, 35.
(78) Reger, D. L.; Little, C. A.; Rheingold, A. L.; Lam, M.; Concolino, T.; Mohan, A.; Long, G. J. *Inorg. Chem.* **2000**, *39*, 4674.
(79) Fallis, I. A.; Farley, R. D.; Malik, K. M. A.; Murphy, D. M.; Smith, H. J. *J. Chem. Soc., Dalton Trans.* **2000**, 3632.

(80) Li, J.; Rafferty, B. G.; Mulley, S.; Proserpio, D. M. *Inorg. Chem*. **1995**, *34*, 6417.

(81) Ierno, H.; Jordanov, J.; Laugier, J.; Greneche, J.-M. *New J. Chem*. **1997**, *21*, 241.

(82) Diebold, A.; Hagen, K. S. *Inorg. Chem*. **1998**, *37*, 215.

(83) Onggo, D.; Scudder, M. L.; Craig, D. C.; Goodwin, H. A. *Aust. J. Chem*. **2000**, *53*, 153.

(84) Constable, E. C.; Baum, G.; Bill, E.; Dyson, R.; van Eldik, R.; Fenske, D.; Kaderli, S.; Morris, D.; Neubrand, A.; Neuburger, M.; Smith, D. R.; Wieghardt, K.; Zehnder, M.; Zuberbühler, A. D. *Chem.*−*A Eur. J.* **1999**, *5*, 498.

(85) Holland, J. M.; McAllister, J. A.; Zhibao Lu; Kilner, C. A.; Thornton-Pett, M.; Halcrow, M. A. *Chem. Commun*. **2001**, 577.

(86) Stassen, A. F.; de Vos, M.; van Koningsbruggen, P. J.; Renz, F.; Ensling, J.; Kooijman, H.; Spek, A. L.; Haasnoot, J. G.; Gütlich, P.; Reedijk, J. Eur. J. *Inorg. Chem*. **2000**, 2231.

(87) Chang, H.-R.; McCusker, J. K.; Toftlund, H.; Wilson, S. R.; Trautwein, A. X.; Winkler, H.; Hendrickson, D. N. *J. Am. Chem. Soc*. **1990**, *112*, 6814.

(88) Szalda, D. J.; Creutz, C.; Mahajan, D.; Sutin, N. *Inorg. Chem.* **1983**, *22*, 2372.

(89) Figgis, B. N.; Kucharski, E. S.; White, A. H. *Aust. J. Chem.* **1983**, *36*, 1537.

(90) Suresh, E.; Venkatasubramanian, K. *Z. Kristallogr*. **1997**, *212*, 239.

(91) Bernarducci, E.; Bharadwaj, P. K.; Potenza, J. A.; Shugar, H. J. *Acta Crystallogr., Sect. C* **1987**, *43*, 1511.

(92) Suh, M. P.; Lee, J.; Han, M. Y.; Yoon, T. S. *Inorg. Chem.* **1997**, *36*, 5651.

(93) Endicott, J. F.; Lilie, J.; Kuszaj, J. M.; Ramaswamy, B. S.; Schmonsees, W. G.; Simic, M. G.; Glick, M. D.; Rillema, D. P. *J. Am. Chem. Soc*. **1977**, *99*, 429.

(94) Roberts, G. W.; Cummings, S. C.; Cunningham, J. A. *Inorg. Chem.* **1976**, *15*, 2503.

(95) Szalda, D. J.; Schwarz, C. L.; Endicott, J. F.; Fujita, E.; Creutz, C. *Inorg. Chem*. **1989**, *28*, 3214.

(96) Caste, M. L.; Cairns, C. J.; Church, J.; Wang-Kan Lin; Gallucci, J. C.; Busch, D. H. *Inorg. Chem*. **1987**, *26*, 78.

(97) Magull, J.; Simon, A. *Z. Anorg. Allg. Chem*. **1992**, *615*, 81.

(98) Hathcock, D. J.; Stone, K.; Madden, J.; Slattery, S. J. *Inorg. Chim. Acta* **1998**, *282*, 131.